Spectroscopy and Photochemistry of Triplet Methylpentadiynylidene (Me−C≡C−C̈−C≡C−H)

Phillip S. Thomas, Nathan P. Bowling, and Robert J. McMahon*

Department of Chemistry, University of Wisconsin, 1101 University Avenue, Madison, Wisconsin 53706

Received March 13, 2009; E-mail: mcmahon@chem.wisc.edu

Abstract: Triplet carbene methylpentadiynylidene, MeC_5H (**1**), was investigated in cryogenic matrices by IR, UV/vis, and EPR spectroscopy. Broadband irradiation ($\lambda > 497$ nm) of the isomeric diazo compounds, 1-diazo-hexa-2,4-diyne (**2**) or 2-diazo-hexa-3,5-diyne (**3**), generates triplet carbene **1**. EPR spectra yield zero-field splitting parameters ($|D/hc| = 0.62$ cm^{-1}, $|E/hc| < 0.0006$ cm^{-1}), which are typical for a triplet carbene with axial symmetry. The electronic spectrum of triplet **1** is characterized by a weak absorption in the near-UV and visible region (350−430 nm) with vibronic progressions corresponding to excitations of the acetylenic stretching and the terminal C≡C−H bending modes. Chemical trapping of triplet **1** in an O_2-doped matrix affords carbonyl oxides derived predominantly from attack at C-3. Upon irradiation at $\lambda > 399$ nm, triplet **1** undergoes photochemical 1,2-hydrogen migration to form hex-1-ene-3,5-diyne (**6**).

Introduction

The chemistry of carbon-rich molecules is a subject of fascination to chemists in a variety of active research areas, including synthetic and mechanistic organic chemistry, astronomy, combustion, molecular spectroscopy, and electronic structure theory. Carbon-rich species are of interest in astrochemistry, as numerous examples have been either detected or postulated to exist in interstellar space and are possibly carriers of the diffuse interstellar bands (DIBS).[1−9] The electronic structure of carbon-chain molecules is a paradigm in computational chemistry and experimental spectroscopy; studies of these molecules give new insights into the nature of chemical bonding.[10−13]

We recently reported the generation and characterization of matrix-isolated triplet HC_5H.[14] Spectroscopic and computational data support a $D_{\infty h}$ structure, with predominant carbene character at C-3, which is also consistent with the chemical reactivity observed between triplet HC_5H and triplet O_2. While this body of data concerning the parent HC_5H appears to be in good harmony, it is not obvious that the picture that emerges is fully commensurate with earlier studies of substituted $R^1C_5R^2$ derivatives. Solution trapping studies of symmetrically substituted species ($R^1 = R^2 = Ph$, CMe_3, $SiMe_3$) afford products derived from reaction at both C-3 and C-1,[15,16] while early spectroscopic studies of monosubstituted derivatives ($R^1 = Ph$, Me, CMe_3; $R^2 = H$) were interpreted exclusively in terms of carbene character at C-1.[17,18] Thus, the need for detailed studies of substituted derivatives of HC_5H became apparent to us. In an effort to bias the inherently symmetrical carbon backbone of triplet HC_5H, we focused the current investigation on MeC_5H (**1**), a monosubstituted derivative that offers the opportunity to enter the potential energy surface via isomeric carbene precursors (Scheme 1). These studies resolve some of the paradoxes concerning structure and spectroscopy of substituted $R^1C_5R^2$ derivatives, provide insight concerning the thermal chemistry and photochemistry for this series of reactive carbon chain species, and corroborate important spectroscopic features of relevance to molecular spectroscopy and astrochemistry.

Results and Discussion

Carbene Precursors. The isomeric diazo compounds, 1-diazo-hexa-2,4-diyne (**2**) and 2-diazo-hexa-3,5-diyne (**3**), serve as photochemical precursors to triplet **1**. Skell and co-workers generated **2** from the corresponding nitroso urea derivative, but

(1) Kaiser, R. I. *Chem. Rev.* **2002**, *102*, 1309–1358.
(2) Ehrenfreund, P.; Charnley, S. B. *Ann. Rev. Astron. Astrophys.* **2000**, *38*, 427–483.
(3) Kaiser, R. I.; Ochsenfeld, C.; Stranges, D.; Head-Gordon, M.; Lee, Y. T. *Faraday Discuss.* **1998**, 183–204.
(4) Maier, J. P. *J. Phys. Chem. A* **1998**, *102*, 3462–3469.
(5) Thaddeus, P.; McCarthy, M. C.; Travers, M. J.; Gottlieb, C. A.; Chen, W. *Faraday Discuss.* **1998**, *109*, 121–135.
(6) Van Orden, A.; Saykally, R. J. *Chem. Rev.* **1998**, *98*, 2313–2357.
(7) Herbig, G. H. *Ann. Rev. Astron. Astrophys.* **1995**, *33*, 19–73.
(8) Thaddeus, P. In *The Diffuse Interstellar Bands*; Tielens, A. G. G. M., Snow, T. P., Eds.; Kluwer: Dordrecht, 1995, pp 369−378.
(9) Jenniskens, P.; Désert, F. X. *Astron. Astrophys., Suppl. Ser.* **1994**, *106*, 39–78.
(10) Fan, Q.; Pfeiffer, G. V. *Chem. Phys. Lett.* **1989**, *162*, 472–478.
(11) Horný, L.; Petraco, N. D. K.; Schaefer, H. F., III. *J. Am. Chem. Soc.* **2002**, *124*, 14716–14720.
(12) Horný, L.; Petraco, N. D. K.; Pak, C.; Schaefer, H. F., III. *J. Am. Chem. Soc.* **2002**, *124*, 5861–5864.
(13) Rogers, D. W.; Matsunaga, N.; McLafferty, F. J.; Zavitsas, A. A.; Liebman, J. F. *J. Org. Chem.* **2004**, *69*, 7143–7147.

(14) Bowling, N. P.; Halter, R. J.; Hodges, J. A.; Seburg, R. A.; Thomas, P. S.; Simmons, C. S.; Stanton, J. F.; McMahon, R. J. *J. Am. Chem. Soc.* **2006**, *128*, 3291–3302.
(15) Hauptmann, H. *Tetrahedron* **1976**, *32*, 1293–1297.
(16) Hori, Y.; Noda, K.; Kobayashi, S.; Taniguchi, H. *Tetrahedron Lett.* **1969**, 3563–3566.
(17) Bernheim, R. A.; Kempf, R. J.; Gramas, J. V.; Skell, P. S. *J. Chem. Phys.* **1965**, *43*, 196–200.
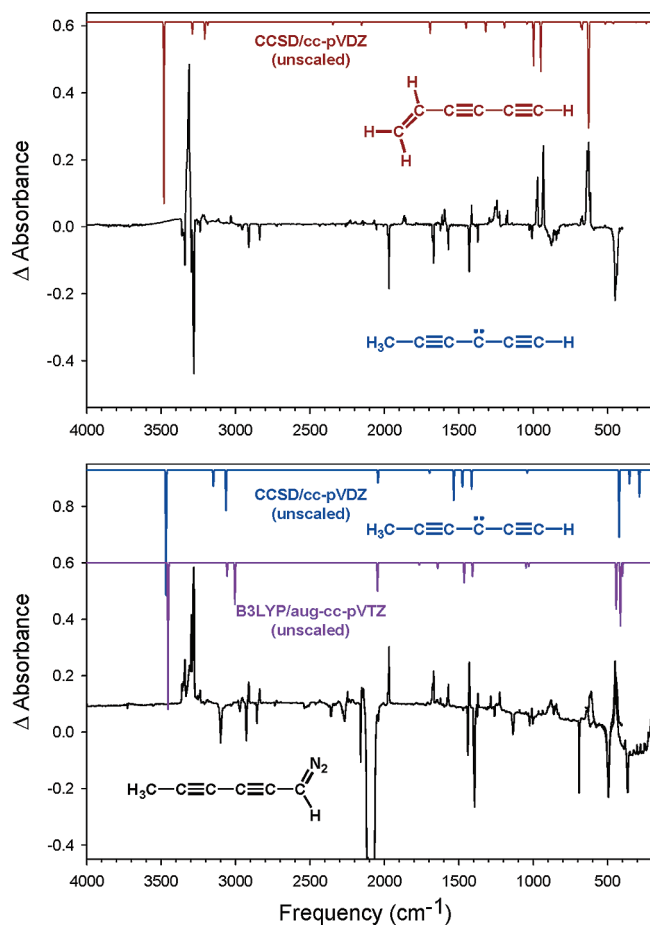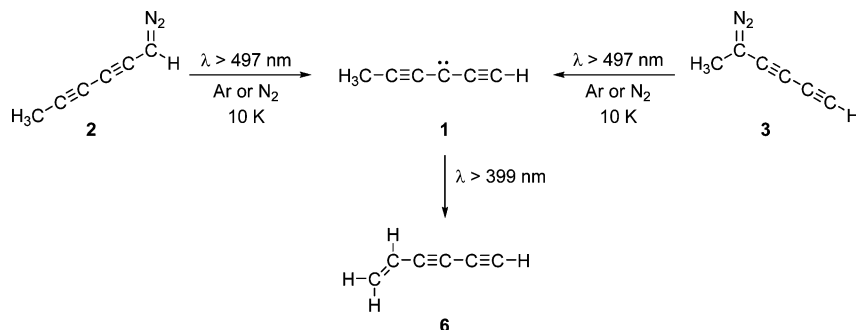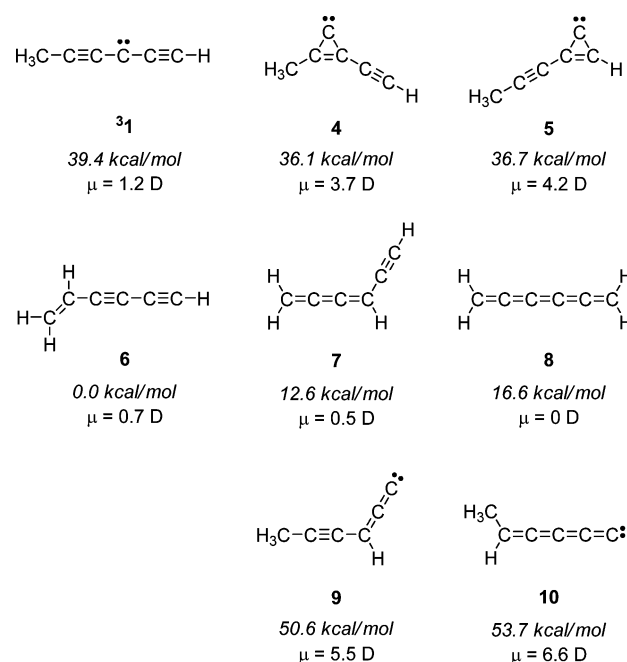(18) Bernheim, R. A.; Kempf, R. J.; Reichenbecher, E. F. *J. Magn. Reson.* **1970**, *3*, 5–9.

Scheme 1. Photochemical Generation and Reaction of Triplet MeC₅H (**1**)

Scheme 2. Computed Relative Energies and Dipole Moments of Selected C₆H₄ Isomers (CCSD/cc-pVDZ)

Figure 1. (Bottom) Experimental IR subtraction spectrum showing the disappearance of diazo compound **2** and growth of triplet MeC₅H (**1**) (N₂, 10 K), in comparison with computed harmonic vibrational frequencies and IR intensities of **1**. The far-IR spectrum (650−200 cm⁻¹) is the result of an independent experiment. (Top) Experimental IR subtraction spectrum showing disappearance of triplet **1** and the appearance of enediyne **6** upon irradiation (λ > 399 nm, 21.2 h) in comparison with the computed spectrum for **6**.

A. IR Spectroscopy. Photolysis of either **2** (λ > 497 nm, 3 h; N₂, 10 K) or **3** (λ > 497 nm, 1.3 h; N₂, 10 K) affords triplet **1** (Figure 1).[20] The experimental IR spectrum displays good agreement with the IR spectra computed for triplet **1** using coupled-cluster (CCSD/cc-pVDZ) or density functional (B3LYP/aug-cc-pVTZ) methods. Detailed spectroscopic assignments will be discussed in the following section. Comparison of the experimental IR spectrum with those computed for other C₆H₄ isomers **4−10** (Scheme 2) establishes that these species are not formed during the visible photolysis of **2** or **3**.[20] It is interesting to note that the product of 1,2-hydrogen migration, hex-1-en-3,5-diyne (**6**), is not observed during the visible-wavelength photolysis of either diazo compound **2** or **3**. This observation was somewhat surprising to us, particularly in the case of diazo compound **3**, because diazo compounds and diazirines that bear a methyl substituent often undergo 1,2-hydrogen migration in the excited state of the carbene precursor or in a vibrationally hot ground-state of the carbene.[21−24]

The observed IR frequencies of MeC₅H (**1**), along with their assignments based on those computed in the harmonic ap-

details of the synthetic procedures and spectroscopic characterization were not published.[17] To the best of our knowledge, the preparation of **3** has not been reported. In the current investigation, we generated diazo compounds **2** and **3** via the Bamford−Stevens rearrangement of the corresponding tosylhydrazone salt. The synthesis of the tosylhydrazones is described elsewhere.[19]

(19) Bowling, N. P.; Burrmann, N. J.; McMahon, R. J. 2009, manuscript in preparation.

(20) Details available as Supporting Information.

(21) LeBlanc, B. F.; Sheridan, R. S. *J. Am. Chem. Soc.* **1988**, *110*, 7250–7252.

(22) Seburg, R. A.; McMahon, R. J. *J. Am. Chem. Soc.* **1992**, *114*, 7183–7189.

Table 1. Experimental and Computed Infrared Frequencies and Intensities for Triplet MeC$_5$H (**1**)[a,b]

1		CCSD/cc-pVDZ		B3LYP/aug-cc-pVTZ		experimental	
mode	symmetry	frequency	intensity	frequency	intensity	frequency	intensity
ω_1	A$_1$	3467	103	3454	119	3278, 3297	100
ω_2	A$_1$	3064	33	3004	34	2838	6
ω_3	A$_1$	2043	10	2046	23	1969, 1977	22
ω_4	A$_1$	1696	2	1765	2	1668, 1675, 1678	16
ω_5	A$_1$	1534	25	1642	5	1569, 1578	10
ω_6	A$_1$	1414	16	1408	11	1373	5
ω_7	A$_1$	1041	0	1049	4	1027	1
ω_8	A$_1$	590	0	599	0.1		
ω_9	E	3149	13	3056	11	2910	10
ω_{10}	E	1476	14	1464	16	1431	21
ω_{11}	E	1040	2	1030	3	1008	6
ω_{12}	E	423	55	414	51	435, 448	94
ω_{13}	E	287	22	442	38		
ω_{14}	E	354	11	401	11	381	5
ω_{15}	E	187	1	204	2		
ω_{16}	E	58	11	89	10		

Other Observed Bands Ascribed to **1**

tentative assignment	frequency	intensity
$\omega_1 + \omega_{16}$	3339, 3351, 3359	32
$\omega_4 + \omega_5$	3254	1
	3237	5
$\omega_3 + \omega_{11}$ or $\omega_5 + \omega_6$	2953	4
	2051	2
$\omega_5 + \omega_{16}$	1622	1
$2\omega_{12}$ or $\omega_{12} + \omega_{13}$	827, 843, 854, 867, 878, 899	57

[a] Harmonic vibrational frequencies (cm^{-1}) and computed intensities (km/mol). Frequencies have not been scaled. *[b]* Experimental intensities reported relative to strongest absorption = 100.

proximation, are given in Table 1. Close inspection of the experimental spectrum reveals that most of the bands are split into two or three peaks, the result of multiple matrix sites. The difficulty in treating this open-shell species, computationally, justifies the comparison of two methods for calculation of the spectrum: Coupled-cluster (CCSD/cc-pVDZ) and DFT (B3LYP/aug-cc-pVTZ) harmonic spectra are utilized to corroborate the assignment of **1**. A few bands are unaccounted for by the calculations: The conglomeration of peaks at 827−899 cm^{-1} appears to be overtone or combination bands of the bending modes observed at 381, 435, and 448 cm^{-1}. These bands appear and disappear in tandem with the other bands of **1** and are recollective of a similar feature in the spectrum of HC$_5$H.[14] Intense overtones and combinations of similar low-frequency bending modes have also been observed in methyldiacetylene[25] and 1-butyne.[26] Three bands are present in the 3339−3359 cm^{-1} region; their relative intensities mimic those for the 3278/3297 cm^{-1} pair, suggesting that the former may be combination bands of ω_1 and ω_{16}. Such an assignment yields a value of ∼56 cm^{-1} for ω_{16}, in accord with the CCSD/cc-pVDZ prediction, but assumes that there is a third band coinciding with the broad peak at 3307 cm^{-1}, which we ascribe to carbene dimer (vide infra). The remaining bands are given tentative assignments as combinations involving the more intense totally symmetric modes ω_3, ω_4, and ω_5 (Table 1).

Dioxiranes (**12b** and **12c**; 1224 and 1285 cm^{-1}) are observed as minor constituents in the spectrum, arising from the reaction of **1** with a trace quantity of oxygen present in the matrix. The assignment of the dioxiranes is based upon chemical trapping studies (vide infra) and computed IR spectra. The remaining IR bands that appear upon photolysis of the diazo compound precursors (2143, 2152, 2247 cm^{-1}, and broad peaks at 639 and 3307 cm^{-1}) are likely due to aggregates or dimers of **1**. (The instability of diazo compounds **2** and **3** necessitates the use of a sample deposition technique that is inherently difficult to control, leading to a less-than-optimal degree of matrix isolation. In our previous study of HC$_5$H, the small quantity of dimer was detectable by UV/vis spectroscopy but not by IR spectroscopy.[14,27])

In an independent experiment, photolysis (λ > 497 nm, 4 h; N$_2$, 9 K) of **2** affords the far-IR portion of the spectrum (650−200 cm^{-1}) that is depicted in Figure 1. Three low-frequency bending modes, ω_{13}-ω_{15}, of **1** are predicted to lie in this region. There is considerable disparity between the two levels of theory in the placement of ω_{13}, one of two high-amplitude terminal C≡C−H wags (the other, ω_{12}, is predicted reliably by both methods). From some experimentation with density functional calculations of varying basis sets, we find that a large basis set (cc-pVTZ or larger) is necessary to converge both C≡C−H bending frequencies. The CCSD/cc-pVDZ frequencies, while reliable for other modes, are probably not converged here. We found previously that some of the bending modes of HC$_5$H also require large basis sets in order to be treated accurately.[14,28] An accurate treatment of the

(23) Jones, M., Jr.; Moss, R. A. In *Reactive Intermediate Chemistry*; Moss, R. A., Platz, M. S., Jones, M., Jr., Eds.; Wiley: Hoboken, NJ, 2004, p 273−328.
(24) Wang, J.; Burdzinski, G.; Gustafson, T. L.; Platz, M. S. *J. Am. Chem. Soc.* **2007**, *129*, 2597−2606.
(25) LaMotte, J.; LaValley, J.; Romanet, R. *J. Chim. Phys.* **1973**, *70*, 1077−1088.
(26) Sheppard, N. *J. Chem. Phys.* **1949**, *17*, 74−78.
(27) Bowling, N. P.; McMahon, R. J. *J. Org. Chem.* **2006**, *71*, 5841−5847.
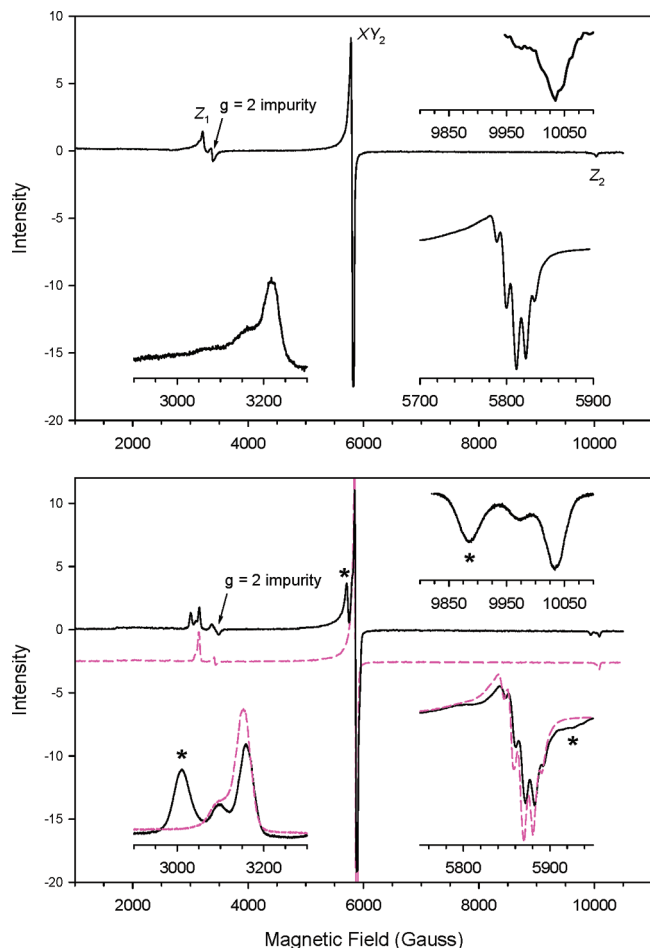(28) Seburg, R. A.; McMahon, R. J.; Stanton, J. F.; Gauss, J. *J. Am. Chem. Soc.* **1997**, *119*, 10838−10845.

Figure 2. (Top) EPR spectrum of triplet MeC$_5$H (**1**) obtained upon irradiation ($\lambda >$ 497 nm, 17.8 h) of 1-diazo-hexa-2,4-diyne (**2**) (Ar, 15 K). (Bottom) Solid line, EPR spectrum of triplet **1**, obtained upon irradiation ($\lambda >$ 472 nm, 15.2 h) of 2-diazo-hexa-3,5-diyne (**3**) (Ar, 15 K); dashed line, EPR spectrum of **1** after warming to ca. 40 K and recooling to 15 K. Transitions of nonrelaxed **1** are designated with an asterisk (*).

C≡C—H bending modes is critical as these bending vibrations appear to account for the vibrational structure of the electronic spectrum of MeC$_5$H (vide infra).

B. EPR Spectroscopy. Figure 2 shows the X-band EPR spectra obtained upon photolysis of **2** and **3** in low-temperature matrices. The spectrum of MeC$_5$H (**1**) is characteristic of an axial triplet and is virtually superimposable on that of HC$_5$H.[14] The large magnitude of the zero-field splitting parameter, $D =$ 0.618 cm^{-1} (Table 2), is characteristic of alkynyl carbenes. Although this value may seem rather large for a species with highly delocalized unpaired spins, it reflects the importance of multiple one-center interactions arising from positive spin density at C-1, C-3, and C-5 and negative spin density at C-2 and C-4 in alkynyl carbenes.[29,30] The small magnitude of the zero-field splitting parameter, $E <$ 0.001 cm^{-1} (Table 2), is consistent with the theoretical prediction of axial symmetry, although the E value must be interpreted cautiously because of the possible influence of molecular tumbling in the matrix.[30]

Expansion of the XY_2 transition reveals splitting similar to that of HC$_5$H, which we previously ascribed to different matrix sites (Figure 2).[14] The observed splitting pattern varies with
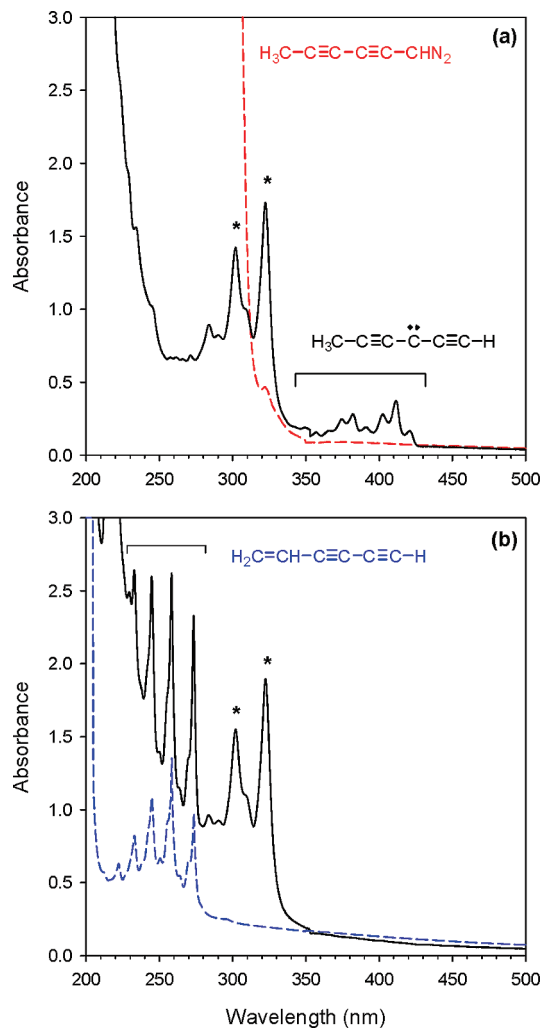
(29) Wasserman, E. *J. Chem. Phys.* **1965**, *42*, 3739–3740.
(30) Seburg, R. A.; Patterson, E. V.; McMahon, R. J. *J. Am. Chem. Soc.* 2009. submitted for publication.

Figure 3. UV/visible spectra. (a) Dash, diazo compound **2** prior to photolysis (N$_2$, 10 K). Solid, triplet MeC$_5$H (**1**) obtained upon irradiation of diazo compound **2** ($\lambda >$ 444 nm, 3.7 h); * = formal carbene dimers. (b) Solid, disappearance of triplet **1** and appearance of enediyne **6** upon irradiation ($\lambda >$ 363 nm, 36 h). Dash, authentic sample of **6** (N$_2$, 10 K).

matrix medium (Ar, N$_2$, methylcyclohexane-d_{14} (MCH-d_{14})), which is consistent with an interpretation in terms of matrix site effects. Although the IR spectra obtained upon photolysis of the isomeric diazo compounds **2** and **3** are indistinguishable, the EPR spectra reveal subtle differences in the photoproducts. Our experience in studying several alkynyl carbenes suggests that loss of dinitrogen from a diazo compound that bears a hydrogen substituent at the diazo carbon, such as **2**, generates a triplet carbene that is apparently able to achieve a relaxed geometry within the matrix site.[14,30−32] This is not to say that the EPR spectrum is devoid of matrix site effects. It is only to say that the spectrum does not exhibit a pronounced change upon annealing the matrix, which would be a characteristic feature of a conformational relaxation process. By contrast, loss of dinitrogen from a diazo compound that bears a substituent at the diazo carbon, such as **3**, generates a triplet carbene for which a portion of the conformational population is not able to

(31) Seburg, R. A.; DePinto, J. T.; Patterson, E. V.; McMahon, R. J. *J. Am. Chem. Soc.* **1995**, *117*, 835–836.
(32) Seburg, R. A.; Patterson, E. V.; Stanton, J. F.; McMahon, R. J. *J. Am. Chem. Soc.* **1997**, *119*, 5847–5856.

Table 2. EPR Data for Triplet MeC5H (**1**)

MeC5H parameter[d]	Ar matrix[a]		N2 matrix[a]	Ar matrix[b]			N2 matrix[b]		MCH-d_{14}[a]	CTFE[a,c]
	site 1	site 2		nonrelaxed	site 1	site 2	nonrelaxed	relaxed		
Z_1	3165	3220	3268	3014	3099	3159	3131	3214	3181	3120
X_2	5797	5804	5801	5711	5855	5864	5877	5877	5720	5796
Y_2	5833	5822	5825	5925	5890	5880	5895	5895	5744	
Z_2	10 035	10 035	10 016	9885	9974	10 034	10 002	10 085		
frequency	9.495	9.495	9.478	9.646	9.646	9.646	9.642	9.642	9.356	9.1536
$\|D/hc\|$	0.6173	0.6189	0.6211	0.6037	0.6115	0.6171	0.6143	0.6221	0.6095	0.609
$\|E/hc\|$	0.0009	0.0004	0.0006	0.0050	0.0008	0.0003	0.0004	0.0004	0.0006	<0.0007

[a] Generated from 1-diazo-hexa-2,4-diyne (**2**). [b] Generated from 2-diazo-hexa-3,5-diyne (**3**). [c] Poly(chlorotrifluoroethylene), ref 18. [d] Magnetic field position (G), microwave frequency (GHz), zero-field splitting parameters (cm^{-1}).

achieve a relaxed geometry within the matrix site.[33−38] The EPR spectrum obtained upon irradiation of **3** exhibits an extra set of transitions, when compared to the spectrum obtained from **2** (Figure 2). These transitions, which we assign as a nonrelaxed conformer of triplet **1**, disappear upon annealing the matrix, with concomitant growth of the transitions of the relaxed carbene.

non-relaxed **1**   relaxed **1**
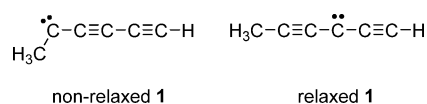
The zero-field splitting parameter, *E*, of the nonrelaxed carbene is significantly larger than that of the relaxed carbene (0.0050 vs 0.0005 cm^{-1}) (Table 2); this value is consistent with a greater deviation from axial symmetry (i.e., a bent structure). After annealing, the spectrum obtained from diazo compound **3** is indistinguishable from the spectrum obtained from diazo compound **2**.

The temperature dependence of the EPR signal of triplet **1** in MCH-d_{14} was measured in the range 4.3−100 K,[20] following the protocol described for triplet HC5H.[14] The observed inverse relationship between signal intensity and temperature (Curie Law) establishes that the triplet state of **1** is either the ground electronic state or that it lies within several cal/mol of the ground state.[39,40]

C. Electronic Absorption Spectroscopy. Photolysis of **2** (λ > 444 nm, 3.7 h; N2, 10 K) generates the electronic spectrum shown in Figure 3. The weak vibronic progression from 345−430 nm is readily attributable to triplet MeC5H (**1**) on the basis of the similarity to the spectroscopic features of triplet HC5H[14] and the correlation the photochemical behavior of this progression with the IR and EPR signals assigned to triplet **1**. In light of the previous uncertainties concerning the electronic spectrum of triplet HC5H,[41,42] the spectrum of MeC5H represents an important result. As only the second example of a triplet R^{1}C5R^2 carbene, it corroborates our recent spectroscopic assignment of HC5H.[14]
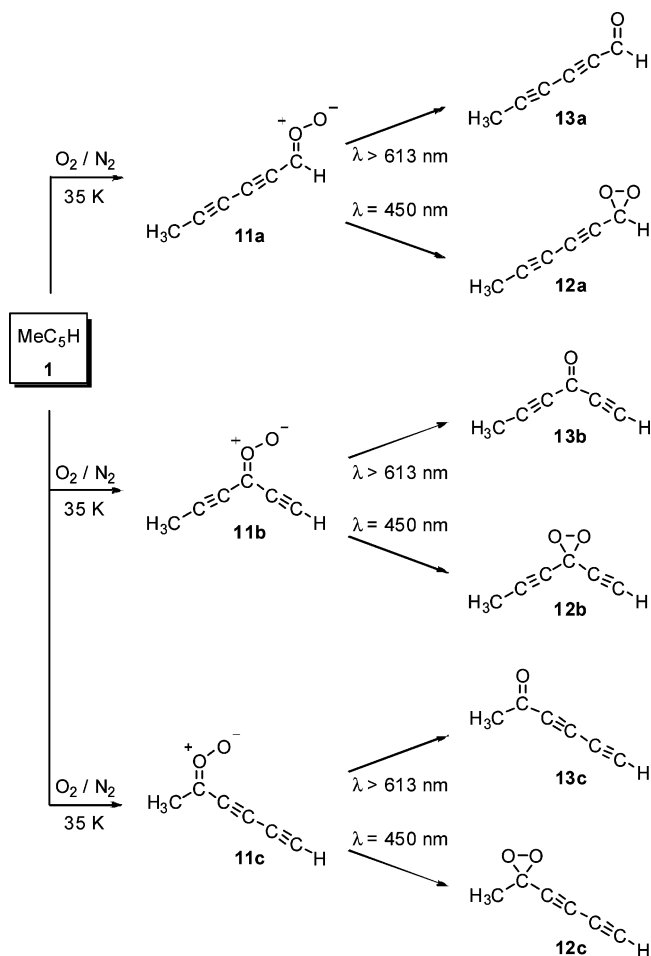
A detailed analysis of the vibronic spectra of HC5H and MeC5H, along with *t*BuC5H and MeC5Me,[43] will be presented elsewhere.[44] The observed progression results from a weakly allowed $A\ ^3A_1 \leftarrow X\ ^3A_1$ transition, which corresponds to an $A\ ^3\Sigma_u^- \leftarrow X\ ^3\Sigma_g^-$ transition in HC5H.[45] Vibronic spacings of ∼1800 and ∼570 cm^{-1} are evident; these frequencies correspond most nearly to carbon−carbon stretching modes in the −C5− chain and terminal C≡C−H bending, respectively. The vibronic structure in **1** is considerably simpler than that of parent HC5H, a trend that is also observed for diacetylene and its substituted derivatives.[46]

The stronger absorption features near 300 and 320 nm (Figure 3) are reminiscent of the formal carbene dimers observed during the photolysis of the parent HC5H.[14] Although these absorptions are prominent in the spectrum, we do not believe that the dimers are present in significant concentration in the matrix. Infrared spectra establish that **1** is the primary species present in the matrix. The extinction coefficients for the dimers are large,[27] rendering them easily detectable by UV/visible spectroscopy.[14]

D. Chemical Trapping Studies. Chemical trapping studies support the spectroscopic assignments for triplet **1**. Most triplet carbenes react readily with O2 to form carbonyl-(*O*)-oxides, which can be photochemically converted to dioxiranes and carbonyl products.[47−49] Our study of triplet HC5H led to the notable finding that HC5H exhibits high selectivity in reacting with O2 at the central carbon (C-3).[14] In the current system, the chemical trapping of **1** with O2 indeed reveals the carbene character of this reactive intermediate. The unsymmetrical substitution pattern, however, complicates the analysis of the regiochemistry of the trapping reaction (Scheme 3). Ultimately, we conclude that reaction of triplet **1** with O2 occurs predominantly at C-3, as described in the following section.

(33) DePinto, J. T.; McMahon, R. J. *J. Am. Chem. Soc.* **1993**, *115*, 12573–12574.
(34) DePinto, J. T.; deProphetis, W. A.; Menke, J. L.; McMahon, R. J. *J. Am. Chem. Soc.* **2007**, *129*, 2308–2315.
(35) Roth, H. D.; Hutton, R. S. *Tetrahedron* **1985**, *41*, 1567–1578.
(36) Noro, M.; Koga, N.; Iwamura, H. *J. Am. Chem. Soc.* **1993**, *115*, 4916.
(37) Noro, M.; Masuda, T.; Ichimura, A. S.; Koga, N.; Iwamura, H. *J. Am. Chem. Soc.* **1994**, *116*, 6179–6190.
(38) Yoshida, K.-i.; Iiba, E.; Nozaki, Y.; Hirai, K.; Takahashi, Y.; Tomioka, H.; Lin, C.-T.; Gaspar, P. P. *Bull. Chem. Soc. Jpn.* **2004**, *77*, 1509–1522.

(39) Wertz, J. E.; Bolton, J. R. *Electron Spin Resonance Spectroscopy*; Chapman and Hall: New York, 1986.
(40) Pryor, W. A.; Hales, B. J.; Premoviv, P. I.; Church, D. F. *Science* **1983**, *220*, 425–427.
(41) Fulara, J.; Freivogel, P.; Grutter, M.; Maier, J. P. *J. Phys. Chem.* **1996**, *100*, 18042–18047.
(42) Ball, C. D.; McCarthy, M. C.; Thaddeus, P. *J. Chem. Phys.* **2000**, *112*, 10149–10155.
(43) Thomas, P. S.; Bowling, N. P.; Burrmann, N. J.; McMahon, R. J. 2009, manuscript in preparation.
(44) Thomas, P. S.; McMahon, R. J. 2009, manuscript in preparation.
(45) Mavrandonakis, A.; Mühlhäuser, M.; Froudakis, G. E.; Peyerimhoff, S. D. *Phys. Chem. Chem. Phys.* **2002**, *4*, 3318–3321.
(46) LaMotte, J.; Binet, C.; Romanet, R. *J. Chim. Phys.* **1977**, *74*, 577–585.
(47) Sander, W.; Bucher, G.; Wierlacher, S. *Chem. Rev.* **1993**, *93*, 1583–1621.
(48) Wierlacher, S.; Sander, W.; Marquardt, C.; Kraka, E.; Cremer, D. *Chem. Phys. Lett.* **1994**, *222*, 319–324.
(49) Sander, W.; Block, K.; Kappert, W.; Kirschfeld, A.; Muthusamy, S.; Schroeder, K.; Sosa, C. P.; Kraka, E.; Cremer, D. *J. Am. Chem. Soc.* **2001**, *123*, 2618–2627.

Scheme 3. Oxygen Trapping of Triplet MeC$_5$H (**1**)

Figure 4. Difference IR spectra of products derived from reaction of triplet MeC$_5$H (**1**) with triplet O$_2$. (Top) Conversion of carbonyl-(*O*)-oxide (primarily **11b**; N$_2$, 10 K) to a mixture of carbonyl-containing products (**13**; peaks designated with ■) and CO upon irradiation at $\lambda > 613$ nm, 0.7 h. (Bottom) In a separate experiment, conversion of carbonyl-(*O*)-oxide (primarily **11b**; N$_2$, 10 K) to dioxirane (primarily **12b**; peaks designated with *) upon irradiation at $\lambda = 450$ nm, 0.7 h. (In both spectra, × = unassigned.)

A matrix containing **1** and 0.43% O$_2$ in N$_2$ was prepared by irradiation ($\lambda > 497$ nm, 10 K) of diazo compound **2**. The sample was annealed (35 K, 5 min) to permit diffusion of dioxygen through the matrix. The matrix turned a bright yellow color, which is characteristic evidence for carbonyl-(*O*)-oxide formation.[14,47−49] The IR subtraction spectrum for this conversion is presented in the Supporting Information, along with computed spectra for the six isomeric carbonyl oxides (**11**). An acetylenic C−H stretching vibration (Figure 4) establishes the formation of **11b** and/or **11c**. The wavelength dependence of the ensuing photochemistry provides additional information concerning the spectroscopic assignments. As established previously, monochromatic irradiation of a carbonyl oxide (ca. $\lambda = 590 \pm 10$ nm) favors cyclization to a dioxirane, while broadband irradiation ($\lambda > 613$ nm) favors O−O bond cleavage to generate a ketone (or aldehyde).[14] Infrared spectra obtained upon irradiation of carbonyl-(*O*)-oxide **11** under these conditions are shown in Figure 4. The conversion of **11** under monochromatic irradiation ($\lambda = 450 \pm 10$ nm) is surprisingly clean, with the formation of only a small amount of carbonyl-containing species (Figure 4). An acetylenic C−H stretching vibration again establishes the formation of dioxirane **12b** and/or **12c**. Careful comparison of the experimental spectrum with the spectra computed for **12a**, **12b**, and **12c** suggests that the sample is comprised largely of dioxirane **12b**. (Each dioxirane is predicted to exhibit two strong IR vibrations in the region 1200−1400 cm^{-1}. The observation of two, and only two, strong vibrations in this region of the experimental spectrum (Figure 4) is thus interpreted in terms of a single predominant species.) The conversion of carbonyl
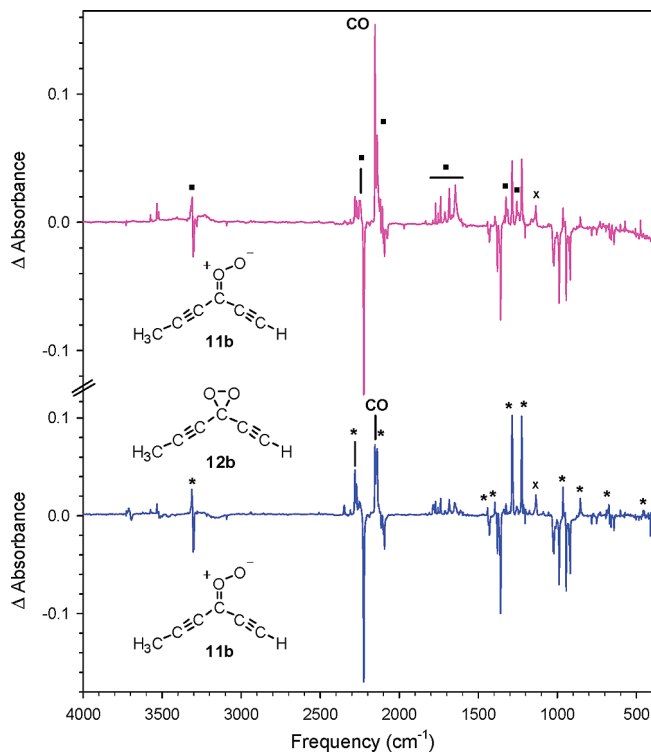
oxide **11** under broadband irradiation ($\lambda > 613$ nm) affords a much more complex product mixture (Figure 4). The proportion of carbonyl-containing products is significantly enhanced, and the proportion of dioxirane **12** is significantly diminished, relative to the experiment involving monochromatic irradiation. Carbon monoxide is also a major product. Further details concerning the comparison of experimental spectra and predicted spectra for dioxiranes **12** and carbonyl compounds **13** are provided in the Supporting Information. In terms of an overall assessment, the IR spectra associated with O$_2$ trapping of MeC$_5$H (**1**) and the subsequent photochemistry of the trapping products appear to be best interpreted in terms of predominant reaction of triplet **1** at C-3. The reactivity parallels that observed previously for triplet HC$_5$H. The sequence involving O$_2$ trapping, carbonyl oxide formation, and photochemistry is fully consistent with that expected for a triplet carbene, thus providing chemical evidence in support of the structural assignment for **1**.

E. Intramolecular [1,2]-Hydrogen Migration. In contrast to the behavior of its unsubstituted analogue (HC$_5$H),[14] triplet MeC$_5$H (**1**) undergoes photochemical rearrangement upon excitation of the $A\,^3A_1 \leftarrow X\,^3A_1$ transition (ca. 400 nm) (Figures 1 and 3). Comparison of the experimental IR spectrum of the photoproduct with spectra computed for 2-ethynyl-3-methyl cyclopropenylidene (**4**), 2-(1-propynyl)cyclopropenylidene (**5**), hexa-1,2-diene-4-yne-1-ylidene (**9**), and hexa-1,2,3,4-tetraen-1-ylidene (**10**) rules out these structures for the photoproduct.[20] Beyond this spectroscopic evidence, per se, the formation of any of these species would be difficult to rationalize in terms of differences in photochemical behavior of substituted (MeC$_5$H) and unsubstituted (HC$_5$H) carbon chains; the methyl substituent

Scheme 4. Possible Hydrogen Shifts in MeC$_5$H (**1**)

Scheme 5. Photochemical Hydrogen-Shift Mechanism in MeC$_5$H (**1**)
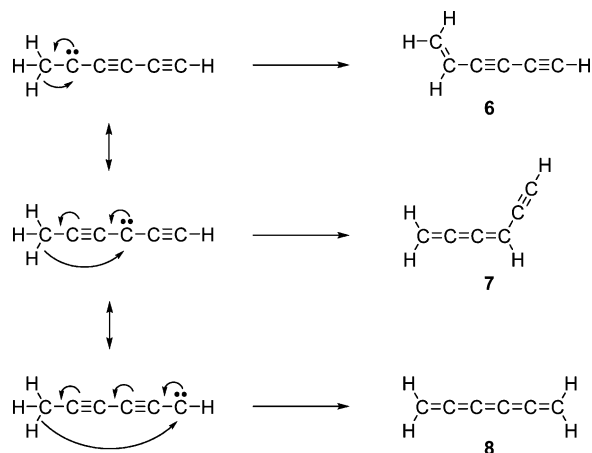
would not play an obvious role in the mechanism of formation of **4**, **5**, **9**, or **10**.

The photochemical process likely involves an intramolecular hydrogen migration reaction - a common thermal and photochemical rearrangement pathway for alkyl-substituted carbenes.[23,50−53] Intramolecular hydrogen shifts typically occur in the closed-shell singlet state. For carbenes with triplet ground states, the singlet state is not appreciably populated at cryogenic temperatures, and, thus, alkyl-substituted triplet carbenes may be thermally stable at low temperatures.[54] The propensity for hydrogen shifts in propargyl carbenes, however, is unclear. In addition to the possibility of a [1,2]-hydrogen migration, we also consider the possibility of [1,4]- and [1,6]-hydrogen migrations in **1** (Scheme 4): (i) earlier product analyses involving RC$_5$R derivatives may be interpreted in terms of carbenic reactivity at C-1, C-3, and C-5 positions,[15,16] (ii) the hydrogen migrations reactions to form **6**, **7**, or **8** are all are highly exothermic (Scheme 2), and (iii) regardless of which species might be first formed from **1**, the initial product might undergo secondary photochemistry under the irradiation conditions.

Extended irradiation of **1** ($\lambda > 399$ nm, 21.2 h) in the weakly allowed $A\ ^3A_1 \leftarrow X\ ^3A_1$ transition (Figure 3) results in the disappearance of the IR, UV/visible, and EPR signals of triplet **1** and appearance of the IR and UV/visible spectra of **6** (Figures 1 and 3). The IR and UV/visible spectra of enediyne **6** were confirmed by comparison with those of an authentic sample.[20] Comparison of the experimental IR spectrum with spectra computed for hexa-1,2,3-triene-5-yne (**7**) and hexapentaene (**8**) rules out the formation of these species.[20] After the complete conversion of **1** to **6**, successive irradiations at shorter wavelengths ($\lambda > 363$ nm, 4.5 h; $\lambda > 328$ nm, 2 h; $\lambda > 280$ nm, 2 h; $\lambda > 261$ nm, 2.7 h; $\lambda > 237$ nm, 13.3 h; $\lambda > 200$ nm, 2 h) effected no change in the observed products.

Photoexcitation of triplet **1** in the weakly allowed $A\ ^3A_1 \leftarrow X\ ^3A_1$ transition (350−430 nm) affords a triplet excited state
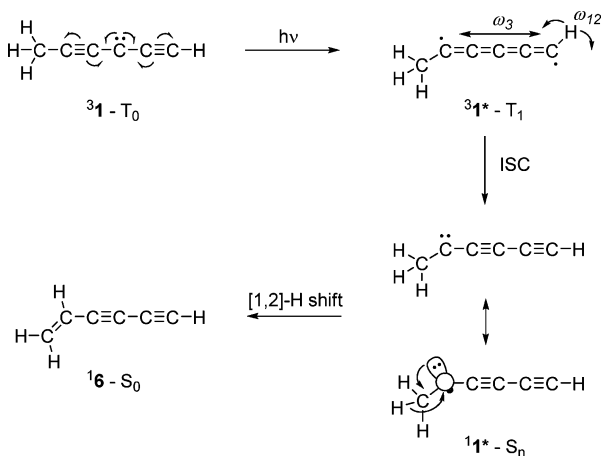
with cumulenic diradical character (Scheme 5).[44] The pathway by which this excited state evolves to the singlet ground state of enediyne **6** remains unclear. It is logical to suggest that the triplet excited state undergoes intersystem crossing (ISC) to singlet **1**, which subsequently undergoes [1,2]-hydrogen migration to afford **6**.[23]

The photochemical rearrangement of triplet **1** is noteworthy in the context of photochemical studies of other alkynyl carbenes. The family of C$_3$H$_2$ isomers exhibits a rich network of photochemical interconversions.[32,55] Triplet HC$_5$H, however, does not exhibit photochemistry at wavelengths accessible to us ($\lambda > 200$ nm; Ar, 10 K)[14]—despite the fact that several other C$_5$H$_2$ isomers are energetically accessible[28] and have been generated and detected in the gas phase.[56−58] The absence of photochemical rearrangement of HC$_5$H may result from an unusually short excited-state lifetime caused by (triplet−triplet) fluorescence or efficient nonradiative deactivation. The photochemical rearrangement of **1** to enediyne **6** establishes that the R^{1}C$_5$R^2 chromophore is not intrinsically unreactive.

We also investigated the propensity for MeC$_5$H (**1**) to undergo a hydrogen migration reaction under thermal conditions. Examples are known in which carbenes undergo intramolecular hydrogen migration either in the triplet ground state via hydrogen atom tunneling, or in a low-lying, thermally populated singlet state.[54] In the case of **1**, IR and EPR spectra do not change upon standing in the dark at 10 K for prolonged periods (63 and 41 h, respectively), establishing the thermal stability of the triplet state under matrix isolation conditions. Annealing carbene **1** in an O$_2$-doped N$_2$ matrix at the modest temperature of 35 K affords oxygen-trapping products (vide supra), but not [1,2]-hydrogen migration product **6**. To enable the use of higher temperatures, we generated **1** in a MCH-d_{14} glass. The parent compound, triplet HC$_5$H, persists in MCH-d_{14} at temperatures up to 80 K but decays at 100 K, presumably via deuterium atom abstraction from the matrix.[14] For triplet **1**, the EPR signal intensity measured at 4 K can be recovered after warming as high as 90 K. Above this temperature, the signal is irreversibly

(50) *Carbenes*; Jones, M.; Moss, R. A., Eds.; R. E. Krieger: Malabar, FL, 1983; Vol. I.

(51) *Carbenes*; Moss, R. A.; Jones, M., Eds.; R. E. Krieger: Malabar, FL, 1983; Vol. II.

(52) *Kinetics and Spectroscopy of Carbenes and Biradicals*; Platz, M. S., Ed.; Plenum: New York, 1990.

(53) Tomioka, H. In *Reactive Intermediate Chemistry*; Moss, R. A., Platz, M. S., Jones, M., Jr., Eds.; Wiley: Hoboken, NJ, 2004, pp 375−462.
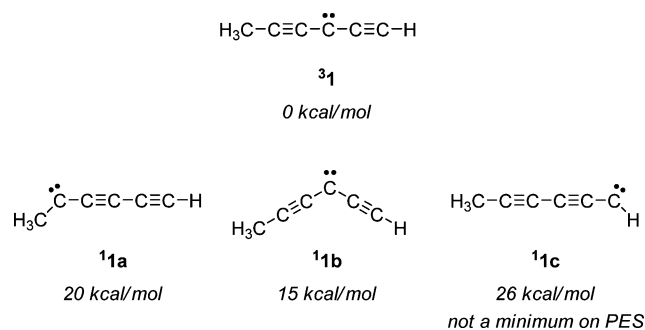
(54) McMahon, R. J.; Chapman, O. L. *J. Am. Chem. Soc.* **1987**, *109*, 683–692.

(55) Maier, G.; Reisenauer, H. P.; Schwab, W.; Cársky, P.; Hess, B. A.; Schaad, L. J. *J. Am. Chem. Soc.* **1987**, *109*, 5183–5188.

(56) Travers, M. J.; McCarthy, M. C.; Gottlieb, C. A.; Thaddeus, P. *Astrophys. J.* **1997**, *483*, L135–L138.

(57) McCarthy, M. C.; Travers, M. J.; Kovacs, A.; Gottlieb, C. A.; Thaddeus, P. *Astrophys. J., Suppl. Ser.* **1997**, *113*, 105–120.

(58) McCarthy, M. C.; Travers, M. J.; Kovács, A.; Chen, W.; Novick, S. E.; Gottlieb, C. A.; Thaddeus, P. *Science* **1997**, *275*, 518–520.

Scheme 6. Computed Relative Energies of MeC$_5$H (**1**) (CCSD/cc-pVDZ)

H$_3$C−C≡C−C̈−C≡C−H

^{3}1

0 kcal/mol

:C−C≡C−C≡C−H   C=C̈...C≡C   H$_3$C−C≡C−C≡C−C:
   H$_3$C   H$_3$C   H   H

^{1}1a   **^{1}1b**   **^{1}1c**

20 kcal/mol   *15 kcal/mol*   *26 kcal/mol*

not a minimum on PES

lost. The close similarity in thermal behavior of HC$_5$H and MeC$_5$H suggests that the thermal, intramolecular [1,2]-hydrogen migration in **1** has not become competitive with bimolecular decay pathways available to the carbene. This situation, in turn, implies a relatively large singlet−triplet energy gap in **1**. By way of comparison, 1-phenylethylidene (PhC̈CH$_3$) undergoes thermal [1,2]-hydrogen migration at an appreciable rate at 60 K in a xenon matrix, which places an upper limit on the singlet−triplet energy gap of ca. 4 kcal/mol.[54,59,60]

In seeking a quantum chemical estimate for the singlet−triplet energy gap in **1**, we considered closed-shell singlet states with carbenic character localized at C-1, C-3, or C-5 (Scheme 6). The lowest-energy singlet corresponds to a carbene structure that is bent at C-3 (^{1}**1b**), although it is not apparent that this state is relevant to the hydrogen shift in question. (Structure ^{1}**1b** exhibits one imaginary vibrational frequency (35i cm^{-1}) associated with methyl torsion; as such, it represents a good approximation to the true minimum on the potential energy surface.) The singlet−triplet splitting is indeed large (ca. 15 kcal/mol). Two nearly degenerate, closed-shell singlets were obtained that correspond to carbene structures that are bent at C-5 (^{1}**1a**). Again, each structure exhibits a single low-frequency imaginary vibration. The singlet−triplet splitting associated with these structures is even larger (ca. 20 kcal/mol). A closed-shell singlet structure corresponding to carbenic character at C-1 (^{1}**1c**) appears not to be a minimum on the potential energy surface.[28] (Structure ^{1}**1c** exhibits three imaginary vibrational frequencies, and optimizes to a structure with a linear C−C−H bond angle.) Our computational estimates for the singlet−triplet energy gap in **1** are thus consistent with the absence of [1,2]-hydrogen migration in **1** upon annealing in MCH-d_{14} at 100 K.

F. Spectroscopy of Isomeric Carbon Chains 1 and 6. Enediyne **6**, the product of [1,2]-hydrogen migration in **1**, is itself a molecule of interest and a plausible interstellar species. Early spectroscopic characterization was accomplished by Böhm-Gössl et al., who obtained the vibrational spectrum of **6** in CCl$_4$ solution and the optical spectrum in methanol and in the gas phase.[61] A well-resolved UV spectrum acquired by Zwier and co-workers via resonant two-photon ionization spectroscopy is also available.[62] Here, we discuss the matrix IR spectrum of **6**, along with assignments and some interpretations regarding its electronic structure.

The experimental spectrum of enediyne **6** is well-replicated by the harmonic frequencies calculated at the coupled-cluster

and DFT levels (Table 3). Most, but not all, of the DFT-calculated fundamental frequencies (which include corrections for anharmonicity) also display excellent correspondence with experiment. The perturbative treatment of anharmonicity fails drastically, however, for the near-degenerate bending modes ω_{13} and ω_{21}. We are also doubtful that the substantial anharmonic contributions computed for ω_{14}, ω_{15}, and ω_{22} are reliable. In the fingerprint region, the experimental spectrum of **6** bears some semblance to that of carbene **1**. The most intense low-frequency modes of **6** (ω_{13}, ω_{21}) are likely responsible for the apparent overtone/combination band system present at 1227−1276 cm^{-1}. On the basis of normal-mode analysis from the calculations, we assign these features to terminal C≡C−H bending vibrations, as we did for **1**.

Comparison of the carbon skeletal modes of carbene **1** and enediyne **6** provides insight into the structure of these molecules. The bending modes of **6** (ω_{13}/ω_{21}, 616, 628, and 638 cm^{-1}) are much stiffer than those of **1** (ω_{12}, 435, 448 cm^{-1}; ω_{14}, < 200 cm^{-1}). The same may be said of the acetylenic C≡C stretching vibrations. On the basis of our assignments, **6** has frequencies of 2228 and 2067 cm^{-1} for in-phase and out-of-phase C≡C stretching, respectively; for **1**, the corresponding frequencies of 1969 and 1668 cm^{-1} more closely resemble typical allenic C=C=C stretching values than acetylenic values.[63] Thus, the carbon backbone of **1** has significant cumulenic bonding character, and is much floppier with respect to bending, whereas the carbon backbone in **6** is well-described as a rigid union of two discrete acetylenic units bound to an ethylene moiety.

With respect to astrochemistry, both triplet **1** and **6** are plausible interstellar molecules. The laboratory rotational spectrum of **6** has been reported by Thorwirth et al.[64] The unsubstituted carbon chain, triplet HC$_5$H, lacks a permanent dipole moment by virtue of its symmetry, and thus does not exhibit a microwave rotational spectrum. Methyl substitution, however, confers a surprising polarity to triplet **1**. Our calculations predict a dipole moment of 1.2 D, suggesting that **1** should be readily detectable in a laboratory discharge by microwave spectroscopy. A variety of structurally related compounds have been detected in space (H−C≡C−C̈−C≡N, HC$_n$ ($n = 1$−8), CH$_3$C$_2$H, CH$_3$C$_4$H),[65,66] supporting the plausibility of triplet MeC$_5$H (**1**) as an interstellar molecule.

G. Computational and Theoretical Studies. Geometrical parameters calculated for triplet MeC$_5$H (**1**) at the CCSD/cc-pVDZ and B3LYP/6-311G* levels of theory are given in Table 4. Qualitatively, both levels of theory predict similar structural features. The carbon backbone displays slightly shorter C−C distances for the bonds between C-1 and C-2, and C-4 and C-5, reflecting contribution from the resonance structure with carbene character at C-3. The differences in bond length along the chain, however, are small, reflecting contributions from other resonance forms. Spin densities and bond orders, computed using Natural Bond Orbital methods, provide additional insight concerning structure and bonding along the carbon chain (Table 5). In accordance with the Mulliken population analysis performed on HC$_5$H,[14] triplet **1** exhibits large spin densities on the central

(59) Sugiyama, M. H.; Celebi, S.; Platz, M. S. *J. Am. Chem. Soc.* **1992**, *114*, 966−973.

(60) Cramer, C. J.; Truhlar, D. G.; Falvey, D. E. *J. Am. Chem. Soc.* **1997**, *119*, 12338−12342.

(61) Böhm-Gössl, T.; Hunsmann, W.; Rohr-Schneider, L.; Schneider, W. M.; Ziegenbein, W. *Chem. Ber.* **1963**, *96*, 2504−2513.

(62) Arrington, C. A.; Ramos, C.; Robinson, A. D.; Zwier, T. S. *J. Phys. Chem. A* **1999**, *103*, 1294−1299.

(63) Bellamy, L. J. *Infrared Spectra of Complex Molecules*; 3rd ed.; Chapman and Hall, Ltd.: London, 1975.

(64) Thorwirth, S.; McCarthy, M. C.; Dudek, J. B.; Thaddeus, P. *J. Chem. Phys.* **2005**, *122*, 184308.

(65) The Cologne Database for Molecular Spectroscopy, www.astro.uni-koeln.de/site/vorhersagen/.

(66) Lovas, F. J. *J. Phys. Chem. Ref. Data* **2004**, *33*, 177−355.

Table 3. Infrared Frequencies and Intensities of Hex-1-ene-3,5-diyne (**6**)^a

	6	CCSD/cc-pVDZ		B3LYP/6-311G*^{b}			experimental	
mode	symmetry	frequency	intensity	frequency	anh.	intensity	frequency	intensity
ω_1	A′	3481	94	3468	3343	99	3312, 3317	100
ω_2	A′	3290	6	3240	3097	10	3210, 3214, 3221	4
ω_3	A′	3207	9	3150	3036	7	3114	2
ω_4	A′	3187	2	3132	2968	11	3031	2
ω_5	A′	2346	1	2316	2272	4	2228	1
ω_6	A′	2153	2	2160	2127	4	2067	1
ω_7	A′	1693	6	1666	1631	7	1611	4
ω_8	A′	1451	3	1457	1428	4	1414	4
ω_9	A′	1319	5	1326	1303	4	1295	1
ω_{10}	A′	1193	3	1211	1196	1	1173, 1180	4
ω_{11}	A′	1042	1	1055	1045	2		
ω_{12}	A′	678	3	692	695	3	671, 680	*4*
ω_{13}	A′	630	40	594	716	41	616, 628, 638	*64*
ω_{14}	A′	515	1	534	776	4		
ω_{15}	A′	461	1	471	807	4		
ω_{16}	A′	240	1	257	272	1		
ω_{17}	A′	106	2	107	110	3		
ω_{18}	A″	998	23	1001	973	20	970, 980	17
ω_{19}	A″	949	26	945	927	45	928, 932	25
ω_{20}	A″	671	4	695	666	5	671, 680	*4*
ω_{21}	A″	626	42	584	718	46	616, 628, 638	*64*
ω_{22}	A″	469	0	496	961	4		
ω_{23}	A″	310	0	326	356	1		
ω_{24}	A″	139	4	140	137	5		

Other Observed Bands Ascribed to **6**		
tentative assignment	frequency	intensity
$2\omega_{13} + \omega_{18}$; $2\omega_{21} + \omega_{18}$; $2\omega_{13} + \omega_{19}$; $2\omega_{21} + \omega_{19}$; $\omega_{13} + \omega_{18} + \omega_{21}$; $\omega_{13} + \omega_{19} + \omega_{21}$	2197	1
$2\omega_{19}$	1858, 1866	5
$2\omega_{13}$; $2\omega_{21}$; $\omega_{13} + \omega_{21}$	1227, 1244, 1258, 1276	19

^{a} Frequencies (cm^{-1}), computed intensities (km/mol), and experimental intensities (relative to the strongest absorption = 100). Intensities computed at B3LYP/6-311G*. ^{b} Correspond to the harmonic frequencies listed.

Table 4. Geometrical Parameters of Triplet MeC$_5$H (**1**)
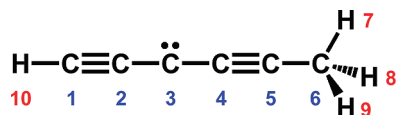
parameter^a	CCSD/cc-pVDZ	B3LYP/6-311G*
R(1,2)	1.2564	1.2397
R(2,3)	1.3289	1.3042
R(3,4)	1.3321	1.3048
R(4,5)	1.2538	1.2405
R(5,6)	1.4713	1.4496
R(6,H)	1.1035	1.0957
R(1,10)	1.0766	1.0631
A(5,6,H)	110.70	111.32

^{a} Bond length (Å), bond angle (°).

and terminal carbon atoms in the −C$_5$− moiety, the largest of which lies on C-3. The effect of methyl substitution is to decrease the spin density on C-5 relative to that on C-1 by hyperconjugative delocalization spin density into the methyl group. Along the carbon chain, bond orders are closer to 1.5 and 2.5 than to 1 and 3; these intermediate values reveal the contribution of cumulenic bonding character.

A more detailed investigation into the electronic structure of triplet **1** is provided by Natural Resonance Theory (NRT) analysis (Figure 5). The dominant resonance structures exhibit three general bonding patterns. The first is an "acetylenic carbene" pattern, which involves two formal triple bonds and a carbene lone pair localized to a single carbon atom. The lone pair may be located on C-1, C-3, or C-5, and as one may predict

from the spin densities (Table 5), the largest weight is assigned to the structure with the lone pair on C-3. The resonance structures involving a lone pair on C-1 or C-5 are not weighted
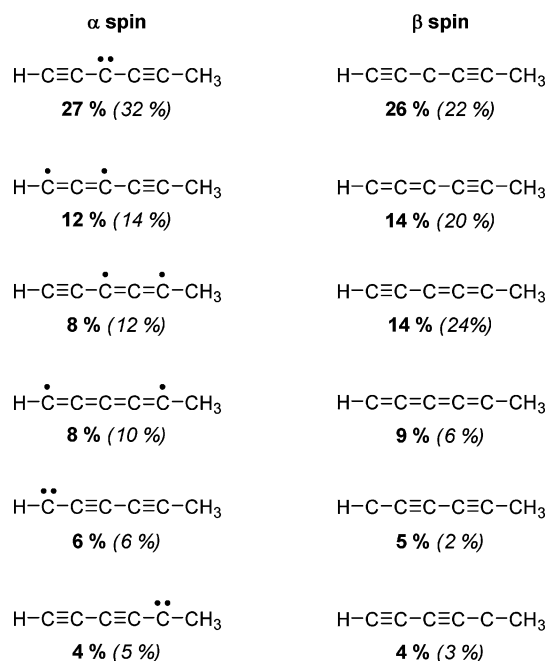

Figure 5. Leading resonance structures of triplet **1** obtained from NRT analysis. CCSD/cc-pVDZ values in bold; B3LYP/6-311G* values in italic.

Table 5. Natural Bond Orbital/Natural Resonance Theory Analysis of Triplet MeC$_5$H (**1**)

				Natural Spin Densities				
atom	H-10	C-1	C-2	C-3	C-4	C-5	C-6	H-7−9
CCSD/cc-pVDZ	−0.034	0.873	−0.384	1.110	−0.367	0.785	−0.050	0.022
B3LYP/6-311G*	−0.030	0.866	−0.309	0.947	−0.295	0.779	−0.045	0.029

				Natural Bond Orders				
	C1−H10	C1−C2	C2−C3	C3−C4	C4−C5	C5−C6	C6−H7	C6−H8,9
				CCSD/cc-pVDZ				
α spin	0.50	1.20	0.71	0.66	1.20	0.56	0.48	0.48
β spin	0.50	1.23	0.69	0.68	1.19	0.5	0.49	0.49
total	1.00	2.43	1.40	1.34	2.39	1.08	0.96	0.97
				B3LYP/6-311G*				
α spin	0.50	1.25	0.72	0.69	1.24	0.54	0.49	0.49
β spin	0.50	1.26	0.71	0.73	1.20	0.54	0.48	0.49
total	0.99	2.50	1.43	1.42	2.43	1.07	0.97	0.97

heavily; their importance is subordinate to more delocalized structures of the second and third types. The second type of structure is characterized by a 1,3-allenic diradical in addition to a formally localized triple bond. Triplet HC$_3$H exhibits a 1,3-allenic diradical structure and a slightly bent geometry.[30,31] The large contribution of this type of resonance structure within the framework of HC$_5$H and MeC$_5$H may serve as an explanation for the soft bending potential of the −C$_5$− chain. Long progressions in low-frequency modes in the electronic spectra of MeC$_5$H and HC$_5$H suggest that the 1,3-allenic diradical resonance structure is significant in describing the excited electronic state responsible for the visible absorption. The final type of bonding pattern is a 1,5-cumulenic diradical, and this represents a smaller overall resonance contribution to the electronic structure of the molecule, as there is only a single contributing form. In addition to the resonance contributors discussed above, the NRT routine found a large number of ionic structures with much smaller weights.

Summary

Triplet MeC$_5$H (**1**) has been generated, under matrix isolation conditions, upon photolysis of either 1-diazo-hexa-2,4-diyne (**2**) or 2-diazo-hexa-3,5-diyne (**3**). IR, UV/visible, and EPR spectra are consistent with the theoretical predication of a molecule with axial symmetry. Although an earlier EPR study was interpreted in terms of a terminal carbene structure (Me−C≡C−C≡C−C̈−H; hexa-2,4-diyn-1-ylidene),[17,18] our spectroscopic, theoretical, and chemical-trapping studies establish that the structure is better depicted as a dialkynyl carbene (Me−C≡C−C̈−C≡C−H; hexa-1,4-diyn-3-ylidene). The electronic absorption spectrum, which exhibits rich vibronic structure, corroborates our recent spectroscopic assignment of triplet HC$_5$H.[14] This result is significant in light of the uncertainty regarding the spectroscopic features of HC$_5$H.[42,67] Unlike HC$_5$H, however, MeC$_5$H (**1**) displays photochemistry. Excitation of triplet **1** in the weakly allowed $A\,^3A_1 \leftarrow X\,^3A_1$ transition results in a [1,2]-hydrogen migration to form enediyne **6**. A thermal [1,2]-hydrogen shift does not occur in an MCH-d_{14} glass at temperatures up to 90 K, suggesting a relatively large singlet−triplet energy gap for MeC$_5$H. NBO calculations on triplet **1** assign a large spin density on the central carbon (C-3) and somewhat smaller spin densities on C-1 and C-5. The bonding within the −C$_5$− chain is characterized by fractional bond orders of 1.5 and 2.5, indicative of a compromise between acetylenic and cumulenic bond patterns. NRT analysis reveals the most

important resonance contributor is a dialkynyl carbene structure (Me−C≡C−C̈−C≡C−H), followed by ethynyl-1,3-allenic diradical and 1,5-cumulenic diradical contributors. Although the large magnitude of the zero-field splitting parameter $D = 0.618$ cm^{-1} may seem rather large for a species with highly delocalized unpaired spins, it reflects the importance of multiple one-center interactions in the dialkynyl carbene **1**.[29,30]

Experimental Section

General. The matrix isolation apparatus and technique have been described previously.[22,68] EPR zero-field splitting parameters were determined by a best fit of the observed spectrum to the spin Hamiltonian utilizing the assumption $g_x = g_y = g_e$.[69]

Computational Methods. Harmonic vibrational frequencies and equilibrium geometries were calculated at the level of CCSD/cc-pVDZ using the Mainz−Austin version of the ACESII program system.[70,71] Vibrational frequencies and geometries calculated using density functional methods (B3LYP/aug-cc-pVTZ, B3LYP/6-311G*, and BLYP/6-31G*) utilized the Gaussian 98[72] and Gaussian 03[73] program suites. NBO and NRT analyses were performed using *NBO 5.G*.[74]

Generation of Diazo Compounds. The syntheses of tosylhydrazone precursors to diazo compounds **2** and **3** are described elsewhere.[19] These tosylhydrazones are stable in a freezer at −20 °C and can be stored for months without significant decomposition. Thermolysis of the corresponding sodium or lithium salts affords the diazo compounds (**2** or **3**). For the purposes of our matrix-isolation experiments, the lithium salts proved to be superior precursors. A small portion of tosylhydrazone (25 mg) was dissolved in Et$_2$O and treated with 1 equiv of *n*-BuLi (in hexanes) at −78 °C. After solvent removal at reduced pressure on a vacuum manifold, the flask containing the lithium salt was attached to the

(67) Fulara, J.; Freivogel, P.; Forney, D.; Maier, J. P. *J. Chem. Phys.* **1995**, *103*, 8805−8810.

(68) McMahon, R. J.; Chapman, O. L.; Hayes, R. A.; Hess, T. C.; Krimmer, H.-P. *J. Am. Chem. Soc.* **1985**, *107*, 7597−7606.

(69) Wasserman, E.; Snyder, L. C.; Yager, W. A. *J. Chem. Phys.* **1964**, *41*, 1763−1772.

(70) Stanton, J. F.; Gauss, J.; Watts, J. D.; Szalay, P. G.; Bartlett, R. J. ACES II Mainz-Austin-Budapest version; www.aces2.de, 2008.

(71) Stanton, J. F.; Gauss, J.; Watts, J. D.; Lauderdale, W. J.; Bartlett, R. J. *Int. J. Quantum Chem.* **1992**, *S26*, 879−894.

(72) Frisch, M. J.; et al. *Gaussian 98, Revision A.6*; Gaussian, Inc.: Pittsburgh, PA, 1998.

(73) Frisch, M. J.; et al. *Gaussian 03, Revision B.05*; Gaussian, Inc.: Wallingford, CT, 2004.

(74) Glendening, E. D.; Badenhoop, J. K.; Reed, A. E.; Carpenter, J. E.; Bohmann, J. A.; Morales, C. M.; Weinhold, F. *NBO 5.0*; Theoretical Chemistry Institute, University of Wisconsin: Madison, WI, 2001.

matrix isolation apparatus and pumped at ~10^{-7} mmHg for 2−4 h to remove residual solvent. The spectroscopic window was cooled to 21 K, and a silicone oil bath (preheated to ca. 80 °C) was placed around the flask to initiate thermolysis of the tosylhydrazone salt. Codeposition of the thermolysate with N_2 afforded the matrix-isolated sample of diazo compound (**2** or **3**). This procedure required a short deposition time (0.5 h) and a fast N_2-deposition rate (1.0−1.5 mmHg/min), because thermal decomposition of the lithium salts occurs relatively rapidly.

1-Diazo-hexa-2,4-diyne (2). IR (N_2, 10 K; relative intensity): 3099 m, 2969 w, 2927 w, 2856 w, 2736 w, 2537 w, 2507 w, 2354 w, 2283 m, 2269 m, 2160 w, 2114 s, 2101 s, 2076 vs, 1472 w, 1438 w, 1393 s, 1371 w, 1259 w, 1133 w, 1024 w, 999 w, 691 w, 615 w, 493 s, 364 m cm^{-1}.

2-Diazo-hexa-3,5-diyne (3). IR (N_2, 10 K; relative intensity): 3307 s, 3222 w, 2965 w, 2942 w, 2600 w, 2205 m, 2195 m, 2188 m, 2160 m, 2068 s, 2053 vs, 2003 w, 1461 w, 1385 w, 1346 w, 1185 w, 1164 w, 1043 w, 1031 w, 660 m, 655 m, 647 m, 581 w, 485 w cm^{-1}.

Supporting Information Available: Details of the preparation of diazo compounds **2** and **3** and synthesis of enediyne **6**; IR data from photolysis of diazo compound **2**; IR spectra of oxygen-trapping experiments; EPR spectra and data from warming/annealing experiments; observed electronic absorption maxima; observed vibrational frequencies; computed vibrational frequencies; Cartesian coordinates and energies of optimized geometries; complete citations for refs 70, 72, 73, and 74. This material is available free of charge via the Internet at http://pubs.acs.org.

JA901977S